Stable ^{15}N and Neutron Halo ^{16}N Nuclei Structure Study by Elastic Electron Scattering Form Factors and Nucleon Momentum Distributions

Stable^{15}N and Neutron Halo ^{16}N Nuclei Structure Study by Elastic Electron Scattering Form Factors and Nucleon Momentum Distributions

Maha Taha Yaseen[1] , Akram M. Ali[2]

1,2 Physics Department, College of Science, University of Anbar, Anbar, Iraq

Email: dr.akram@uoanbar.edu.iq

Abstract. In this manuscript, the elastic electron scattering form factors and the nucleon momentum distributions (NMD) for stable ^{15}N and neutron halo ^{16}N at the ground state were reported. This was accomplished by utilizing the well-known Coherent Density Fluctuation Model (CDFM) via the employment of fluctuation function ($|F(q)|^2$) which is coupled with the density distributions nuclei. The long-tail performance in the NMD at high momentum region was further determined via experimental and theoretical fluctuation functions. The evaluated elastic electron scattering form factors were evaluated on the bases of the density distributions as well as the root mean square (RMS) radii for each measured nucleon. The proposed study provides a robust correlation between the theoretical formation factors and the practical results of ^{15}N and ^{16}N nuclei.

Keywords: CDFM, ^{15}N and ^{16}N, density distributions, RMS radii

1. Introduction

The elastic electron scattering, the density distributions, as well as RMS radii are considered as the most fundamental quantities, which provide insights about the inner structure of both neutron and proton. These together are known as nucleons [1-4]. Recently, several approaches have been proposed for the sole purpose to determine the aforementioned quantities. A typical example of this is the discovery of the halo phenomenon in the stable and exotic nuclei [4, 5]. In the case of stable nuclei, the elastic electron scattering is to be considered a dominant quantity for investigating the nuclear structure. This can be mainly attributed to the interaction of electron with nucleus which is attained via electromagnetic interaction [3]. Generally, a halo nucleus, since its discovery in 1985, possesses large neutron and proton excess whereby the bounds of few outer nucleons are considered weak [6]. The halo nature of a nucleus is principally caused by a specific effect which in turn can be attributed to a continuum close bound state. The essential requirements for the occurrence of a halo are short-range interaction, relatively low angular momentum and low binding energy [7]. A neutron halo is not limited to the unstable nuclei, however, it is usually observed in exotic nuclei on a large-scale as compared to the stable nuclei. The neutron halo could also be perceived off the β-stability line [8]. The previous studies reported that several ground state nuclei possess a halo structure, which is in a close position to the drip-line. These halos can be one-neutron halo (11Be and 19C), two-neutron halo (14Be, 11Li, and 6He), three-neutron halo (26F) and four-neutron-halo (8He) [9-15]. Moreover, the valence neutron can be channeled into the space near the nuclear core so that the neutron is extended with some distance. This distance is estimated to be of higher value as compared to the typical nuclear radius. Therefore, the angular momentum may have some influence on the halo formation which in turn leads to a probability of the s-state to be outside the core's potential range [6, 16, 17]. However, the pandd-states possess much lower probability to form a halo structure due to the relatively large centrifugal barrier[18].

As such, a number theoretical attempts were proposed to investigate the elastic electron scattering form factors as well as the NMD. Karataglidis and Amos [19] demonstrated the transverse and longitudinal form factors from isotopes such as He, Li, and 8Bi. Roca-Maza et al. reported a systematic investigation regarding the elastic electron scattering of both unstable 36Ca and stable 40Ca nuclei using the phase-shift analysis model [20]. Another research group supervised by Chu, Y. et al, also considered the elastic electron scattering of S and O isotopic chains in which they stated that the phase-shift analysis model is capable of reproducing the data obtained experimentally for both heavy and light nuclei [21]. Lately, Hamodi et al. revealed the calculation of the NMD and elastic electron scattering for odd and even p-shell nuclei using CDFM [22]. In this theory, which is an original effort of Antonov et al.[23], the NMD as well as nucleon density distributions (NDD) can only be linked and consequently expressed of the available weight function, $|f(x)|^2$, obtained experimentally. The same research group examined the NMD of some stable and unstable nuclei (4He, 16O, 12C, 40Ca, 39K, and 48Ca) expressed via weight function by means of NDD using the two-parameter fermi (2pF) model [24, 25]. The elastic electron scattering and NMD were observed for 1p-shell, sd-shell, as well as fp-shell nuclei through the CDFM framework [2, 26, 27]. Another study conducted by Ridha et al. reported the investigation of the NDD and elastic charge form factors of 11Be, 19C, 11Li, 8B, 17Ne, 4He, 12C and 16O nuclei using Woods Saxon single-particle radial wave function. The outcomes were compared with harmonic-oscillator potential [28-31]. They found that the utilized Wood Saxon single-particle wave function is in a good agreement with stable and exotic nuclei experimental data. In the same framework, the NDD was also examined alongside the elastic electron scattering for 48Ca and 40Ca nuclei[32]. In this attempt, the study is conducted to explore the elastic electron scattering form factors, density distributions, and RMS radius of stable 15Nandneutron halo 16N nuclei via neutron halo outside the core utilizing two approaches namely CDFM and 2pF.

2.Theory

A single body operator's NDD can be expressed as demonstrated in Equation (1).

$$\rho(r) = \frac{1}{4\pi}\sum_{nl} \xi_{nl}\, 4(2l+1)|R_{nl}|^2 \quad (1)$$

whereby the state $n\ell$ nucleon occupation probability is represented byξ_{nl}, (closed-shell nuclei: $\xi_{nl} = 0\ or\ 1$; and open-shell nuclei:$0 < \xi_{nl<1}$), while R_{nl} is the single-particle harmonic oscillator wave functionradial part.

The NDD of 15N and 16N nuclei represented at the 2s1d-shell end is derived based on a particular hypothesis by which an occupied shell core is existed (1s as well as 1p) and the nucleon occupation numbers in 2s and 1d shells are equal to (4-α), and (A-20+α1), respectively. Meanwhile, it is in a simple shell model (4) and (A-20). Using this assumption with Equation (1), the form of the analytical NDD is given as:

$$\rho(r) = \frac{exp(-R^2/b^2)}{\pi^{3/2}b^3}\left\{10 - \frac{3}{2}\alpha_1 + 2\alpha_1(\frac{r}{b})^2 + (\frac{4A}{15} - \frac{8}{3} - \frac{2\alpha_1}{5})(\frac{r}{b})^4\right\} \quad (2)$$

Herein, the mass number is represented by the letter A, while b is the size parameter, α1 describes the occupation numbers deviation of the nucleon from the shell model where α1=0 and α2 are presumed as an uncontrolled parameter which must be adjusted to have a covenant alongside the regarded NDD experimental measurements. Herein, the normalization condition of ρ(r) can be expressed as [31].

$$N = 4\pi\int_0^\infty \rho(r)r^2dr \quad (3)$$

The RMS radii of the nuclei is expressed as follow [31]:

$$< r^2 >^{1/2} = (\frac{4\pi}{N}\int_0^\infty \rho(r)r^4dr)^{1/2} \quad (4)$$

At central density$\rho(r) = 0$, the NDD at the nucleus center from Equation (2) is given as:

$$\rho(0) = \frac{1}{\pi^{3/2}b^3}\left(10 - \frac{3}{2}\alpha_1\right) \quad (5)$$

so α_1 becomes:

$$\alpha_1 = \frac{2}{3}\left(10 - \rho(0)\pi^{3/2}b^3\right) \quad (6)$$

By substituting Equation (2) into Equation (4) with some simplification:

$$\langle r^2\rangle = \frac{b^2}{A}\left(\frac{9A-120}{2} + \alpha_1\right) \quad (7)$$

herein, the central density $\rho(0)$ and $\langle r^2\rangle$ values are obtained using the experimental values whereas the parameter b is nominated to duplicate the RMS radii of a nucleus obtained experimentally.

The NMD, n(k), of the nuclei is considered via two different models. One of which is calculated using the shell model through single-particle harmonic oscillator wave functions in momentum demonstration, and it is assumed using Equation (8) [31]:

$$n(k) = \frac{b^3}{\pi^{3/2}} \exp(-b^2k^2)\left(10 + 8(bk)^4 + \frac{8(A-40)}{105}(bk)^6\right) \quad (8)$$

where the symbol k- represents the particle momentum.

In the meanwhile, the second model (NMD) is considered using the CDFM, whereby Equation (9) represents the mixed density [33, 34].

$$\rho(r,r') = \int_0^\infty |f(x)|^2 \rho_x(r,r')dr \quad (9)$$

herein a density matrix for A nucleon distributed equivalently at radius x of the sphere can be given by [11]:

$$\rho_x(r,r') = 3\rho_0(x)\frac{j_1\left(k_{F(x)}|r-r'|\right)}{k_F|r-r'|}\theta\left(x - \frac{1}{2}|r-r'|\right) \quad (10)$$

where the density is$\rho_0(x) = 3A/4\pi x^3$;kF is the Fermi momentum, given as [35]:

$$k_F(x) = \left(\frac{3\pi^2}{2}\rho_0(x)\right)^{1/3} = \left(\frac{9\pi A}{8}\right)^{1/3}\frac{1}{x} = \frac{\alpha}{x} \quad (11)$$

and θ is the step function ($\theta = 0\ or\ 1$). Equation (9) corresponds to an equation in a CDFM because the nuclear material fluctuates and tries to maintain the spherical shape of the nucleus and its symmetry.

The density of the single-particle based on the diagonal element of Equation (9) can be expressed as presented in Equation (12) [34]:

$$\rho(r) = \rho_x(r,r'=r)\int_0^\infty |f(x)|^2\rho_x(r)dx) \quad (12)$$

where $\rho_x(r) = \rho_0(r)\theta\ (x-r)$ and the weight function can be expressed as presented in Equation (13) [23, 34]:

$$|f(x)|^2 = \frac{-1}{\rho_0(x)}\frac{d\rho(r)}{dr} \quad (13)$$

The NDD is then calculated with respect to the normalization condition:$\int_0^\infty |f(x)|^2 = 1$.

According to Equation (12) the nucleon momentum distribution can be given as [33, 34]:

$$n(k) = \int_0^\infty |f(x)|^2 n_x(k)dx \quad (14)$$

where the Fermi -momentum distribution of all nucleons is given as,

$$n_x(k) = \frac{4}{3}\pi x^3\theta(k_F(x) - |k|) \quad (15)$$

and using weight function and Equations (13 and 14) the nucleon momentum in CDFM can be expressed as:

$$n_{CDFM}(k) = \left(\frac{4\pi}{3}\right)^2\frac{4}{A}\left[6\int_0^{\alpha/k}\rho(x)x^5dx - \left(\frac{\alpha}{k}\right)^6\rho\left(\frac{\alpha}{k}\right)\right] \quad (16)$$

With a normalized condition: $A = \int n_{CDFM}(k)\frac{d^3k}{(2\pi)^3}$.

For the target nucleus form factor F (q), the expression in coherent density fluctuation model can be given as [33, 34]:

$$F(q) = \frac{1}{A}\int |f(x)|^2 F(q,x)dx \quad (17)$$

Where the uniform charge density distribution is represented as F (q, x) that reflects the scattering event in CDFM with amplitude is a superposition of all charge distribution, which can be expressed as,

$$F(q,x) = \frac{3A}{(qx)^2}\left[\frac{\sin(qx)}{(qx)} - \cos(qx)\right] \quad (18)$$

Equation (18) must be multiplied by a correction of free nucleon finite-size form factor (same protons and neutrons) and center of mass form factor. This eliminates the false state appears from the indication of the mass center. These form corrections can be expressed as follow [31]:

$$F_{fs}(q) = \exp\left(\frac{-0.43q^2}{A}\right)\ and\ F_{cm}(q) = \exp\left(\frac{b^2q^2}{4A}\right) \quad (19)$$

The weight function ($|f(x)|^2$) is obtained using the estimatedNDDfrom2pF model by which the experimental elastic electron scattering was utilized as an input quantity. Consequently, the theoretical value of the mention elastic electron scattering was also used as a comparison point.

Wood-Saxon function for the density of 2pF is given by [27]

$$\rho_c(r) = \frac{\rho_0}{1+\exp(r-c/z)} \quad (20)$$

So, the weight function will be:

$$|f(x)|^2 = \frac{4\pi x^3 \rho_0}{3Az}(1 + \exp(x - c/z))\exp(x - c/z) \qquad (21)$$

If Equation (2) inserted into the equation of weight function (13), an analytical expression cab be acquired as,

$$|f(x)|^2_{2pF} = \frac{8\pi x^4 \rho(x)}{3Ab^2} - \frac{16x^4}{3A\pi^{1/2}b^5}\left\{\left[\alpha_1 + \frac{4A}{15} - \frac{8}{3} - \frac{2\alpha_1}{5}\right](\frac{x}{b})^2\right\} \qquad (22)$$

3. Results and discussion

Table 1: The parameters used in the determination of nuclear density.

Nucle i	c (fm)	z (fm)	b (fm)	$\rho(0)$ (fm^{-3})	α_1
^{15}N	2.638	0.520	1.710	0.2698	1.6586
^{16}N	2.692	0.523	1.72	0.2673	1.7050

3.1 Root *mean square* radii

The proton, neutron (R_p and R_n) and the matter RMS radii of the core and halo are generally evaluated using the harmonic oscillator radial wave function potential or radial wave function of Wood-Saxon potential, respectively. The R_p and R_n matter RMS radii obtain educing Equation (4) are summarized in Table (2). As presented in Table (2), the R_p, R_n matter RMS radii exhibited small differences in^{15}N and ^{16}N nuclei. It is noteworthy mentioning that the only input in the utilized densities calculation is the matter radii(R_m).Table (2) tabulates the calculated charge RMS radius for both ^{15}N and ^{16}N nuclei with the corresponding available experimental values using previously published data [36]. The obtained results of ^{15}N are in an upright agreement with the reported data, while the evaluated values of ^{16}N RMS radius are relatively smaller.

Table 2: RMS radius values of proton and neutron compared with experimental data.

Nuclei	RMS radius(fm)		RMS present work	
	Present work	Experimental	Proton	Neutron
^{15}N	2.426	2.42∓0.10 [36]	2.4084	2.431
^{16}N	2.479	2.50∓0.10 [36]	3.743	3.85

3.2 Density distributions

The density distributions analysis of both ^{15}N and ^{16}N nuclei are presented in this section using 2pF model, as expressed in Equation (20). The main reason for these nuclei to be selected is the unavailability of experimental density distributions data[24]. In the current study, the density distributions is calculated based on two parameters one of which is nucleus radius (c), while another is the skin thickness (z). The NDD is based primarily on the (c) value, particularly when the value of (c)is greater than the nuclei RMS radius. Herein, the (c) value rises as the mass number increases, particularly when the nuclear core and halo skin thicknesses are considered constant. This can be clearly observed from Table (1) and (2).

The ^{15}N nucleus density distributions were presumed through the consideration of the nucleus as a core and consequently evaluating its density distribution; assuming to be of similar shape to the Wood-Saxon alongside the 0.65 fm as the diffuseness parameter. The signal-neutron wave function can be estimated through solving Schrodinger formula which in turn can be solved using Wood-Saxon and/or Coulomb potentials; this can be advantageous in attaining a precise separation energies of the neutron, which corresponds to 1p, 2s as well as 1d orbitals. The total density distributions were obtained by adding the so-called nucleus as a core and the wave function parts. Similarly, 16N analysis was conducted assuming that a single neutron and 15N core are composed.

The distribution of the cores was noticed to be practically indistinguishable. The 15N and 16N density distributions are very alike, yet the single-neutron of 15N ranges was found to be considerably high-spaced because of the relatively small separation energy of the neutron (0.108 MeV). It should be mentioned that the corresponding energy separation of the neutron value for 16N being 0.248 MeV. Figure 1 (a and b) illustrates the NDD for both 15N and 16N nuclei as a function of the distance (r) in fm. The solid curves in Figure 1 are calculated theoretically using Equation (2), while the dotted curves are the experimental NDD data of the 2pF. The two curves showed the same behavior in falling as r increases in the region of the single-neutron.

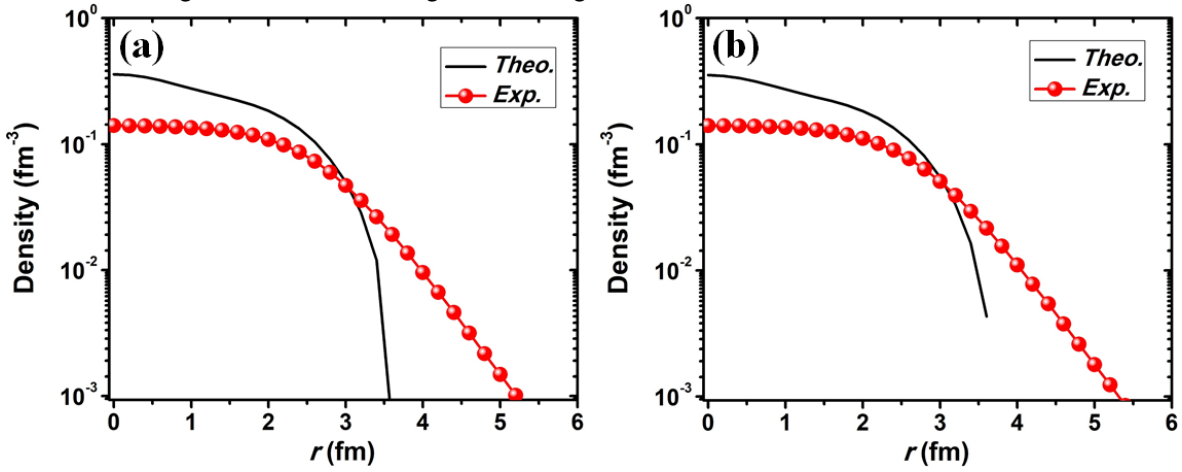

Figure 1: The evaluated nucleon density distributions for both ^{15}N (a) and ^{16}N (b) nuclei. The core ^{15}N is considered for ^{16}N, while the halo single-neutron is represented separately. The experimentally obtained nucleon density distributions are also presented using 2pF model.

3.3 Nucleon momentum distributions

To calculate the NMD, the CDFM model is used as expressed in Equation (16). In Figure 2 (a and b), the NMD is plotted as a function of the momentum $k(fm^{-1})$for ^{15}N and ^{16}N nuclei, respectively. The NMD dotted and solid curves are evaluated using theoretical and experimental weight function $|f(x)|^2$, respectively. It is worth mentioning that the general performance of the NMD at regions of high momentum ($k \geq 2$ fm^{-1}) for both ^{15}N and ^{16}N nuclei are similar; whereby the mentioned distributions possess the properties of a long-tail which are in a well agreement with other reported studies [27-30]. The long-tail in Figure (2), attained using CDFM, is correlated with that of high densities $\rho_x(r)$, Equation (12). This particular hypothesis concludes that ^{15}N and ^{16}N nuclei fluctuation function $|f(x)|^2$ is relatively minor, and these outcomes are in an upright agreement with other data obtained experimentally [25].

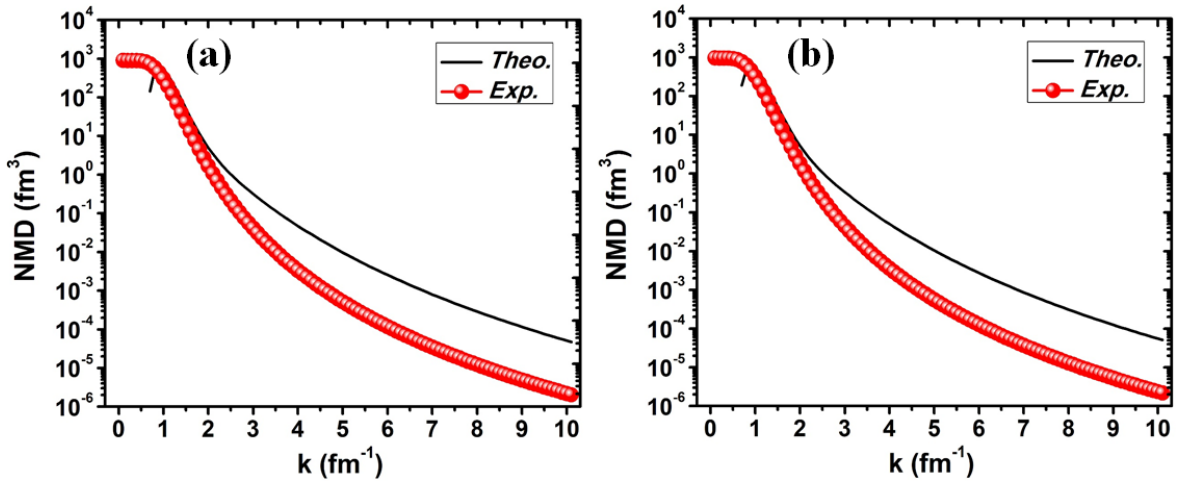

Figure 2: The NMD versus *k* for ^{15}N "(a) and ^{16}N (b) nuclei. The curve with red circles is the evaluated NMD which is expressed using CDFM, while the black solid curve is the evaluated NMD using Equation (8).

3.4 Elastic form factors

The nuclei electron scattering quantity provides good insights about the nucleus charge and size distributions. The presented results in Figure 3, calculated in the framework of CEDM according to Equation (18), are plotted as a function of momentum transfer q (fm^{-1}) for ^{15}N and ^{16}N nuclei. The solid as well as dotted curve in Figure 3 (a and b) are the evaluated results with the correction form included and excluded of the finite-size nucleon and mass center using Equation (19), respectively. Elastic form factors experimental data are plotted as solid circles for the considered nuclei. Figure 3 (a and b) elucidates the form factors obtained experimentally of ^{15}N and ^{16}N nuclei which are considered to be in good agreement with those obtained theoretically. The corrections of the form factor (red dotted curve) showed a slight reduction in comparison to the presented calculation prior to the corrections (solid black curve). The presented correction of the form factor is closer to the experimental values.

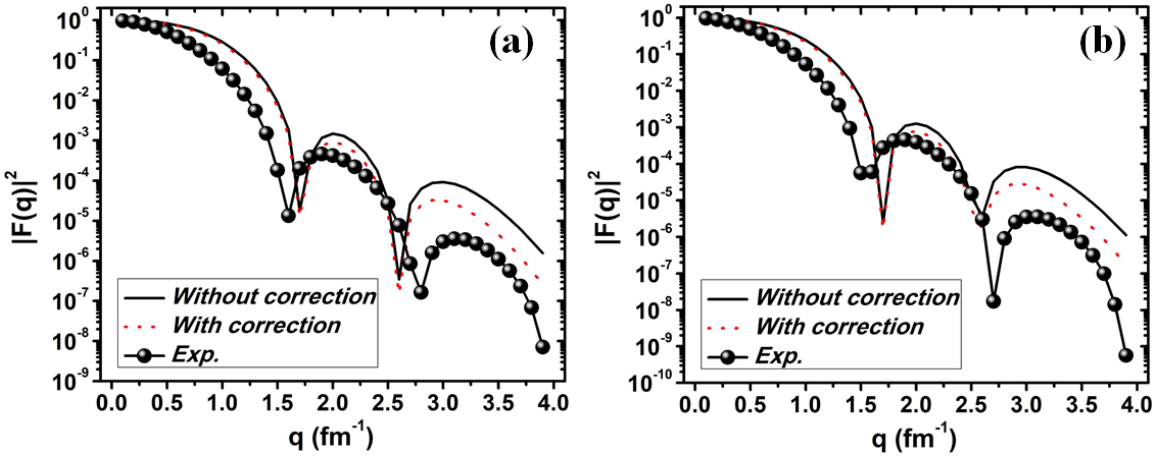

Figure 3: The charge form factors squared for elastic electron scattering for ^{15}N (a) and ^{16}N (b) nuclei as a function of the momentum transfer.

4.Conclusion

In the present study, the charge density distributions using 2pF model for ^{15}Nand ^{16}N were reported. Furthermore, using the obtained density distributions, the form factors were also evaluated which in turn suggested that the form factor depends on the density distributions and RMS radii. It was observed from the current investigation that the differences between neutron and proton RMS radii for each nuclei are small which agreed with experimental data. The ground state nucleon and matter densities of stable ^{15}N and exotic neutron halo nuclei ^{16}N were estimated using the CDFM. The long-tail feature performance at the high momentum region of the NMD was demonstrated utilizing both experimental and theoretical weight functions. The perceived nuclei electron scattering form factors in the current study are well-reproduced using the current evaluation throughout the momentum transfer value (q).

References

[1] Punjabi, V., Perdrisat, C. F., Jones, M. K., Brash, E. J., & Carlson, C. E. (2015). *Eur. Phys. J. A*, **51**(7) 79.
[2] Hamoudi, A. K., Hasan, M. A., & Ridha, A. R. 2012 *Pramana*, **78**(5) 737
[3] Donnelly, T. W., & Sick, I. 1984 *Rev. Mod. Phys.* **56**(3) 461.
[4] Abdullah, A. N. (2017). *Pramana*, **89**(3) 43.
[5] Ozawa, A., Suzuki, T., & Tanihata, I. 2001 *Nucl. Phys. A*, **693**(RIKEN-AF-NP-384) 32
[6] Phookan, C. K. (2014). *A Thesis* (Doctoral dissertation, GAUHATI UNIVERSITY).
[7] Jensen, A. S., & Riisager, K. (2000). *Phys. Lett. B*, **480**(1-2) 39
[8] Ogloblin, A. A., Danilov, A. N., Belyaeva, T. L., Demyanova, A. S., Goncharov, S. A., & Trzaska, W. (2011). *Phys. Rev. C*, **84**(5) 054601.
[9] Fukuda, M., Ichihara, T., Inabe, N., Kubo, T., Kumagai, H., Nakagawa, T., ... & Kouguchi, M. (1991). *Phys. Lett. B*, **268**(3-4) 339
[10] Bazin, D., Brown, B. A., Brown, J., Fauerbach, M., Hellström, M., Hirzebruch, S. E., ... & Powell, C. F. (1995). *Phys. Rev. lett.* **74**(18) 3569.
[11] Tanihata, I., Hamagaki, H., Hashimoto, O., Shida, Y., Yoshikawa, N., Sugimoto, K., ... & Takahashi, N. 1985 *Phys. Rev. lett.* ***55*****(**24) 2676.
[12] Tanihata, I., Kobayashi, T., Suzuki, T., Yoshida, K., Shimoura, S., Sugimoto, K., ... & Wieman, H. 1992 *Phys. lett. B*, **287**(4) 307
[13] Labiche, M., Orr, N. A., Marqués, F. M., Angélique, J. C., Axelsson, L., Benoit, B., ... & Clarke, N. M. 2001 *Phys. Rev. lett.* **86**(4) 600.
[14] Zhukov, M. V., Korsheninnikov, A. A., & Smedberg, M. H. 1994 *Phys. lett. C*, **50**(1) R1.
[15] Ren, Z., Chen, B., Ma, Z., Zhu, Z., & Xu, G. 1996 *J. Phys. G Nucl. Part. Phys.* **22**(4) 523.
[16] Hansen P., Jonson B. 1987 *Eur. Lett.* **4** 409
[17] Hansen, P. G., Jensen, A. S., & Jonson, B. 1995 *Annu. Rev. Nucl. Part. Sci.* 45(1) 591
[18] Li, E. T., Guo, B., Li, Z. H., Wang, Y. B., Li, Y. J., Wu, Z. D., ... & Fan, Q. W. 2016 *Chinese Phy. C*, **40**(11) 114104.
[19] Karataglidis, S., & Amos, K. 2007 *Phys. Lett. B*, **650**(2-3) 148
[20] Roca-Maza, X., Centelles, M., Salvat, F., & Vinas, X. 2008 *Phys. Rev. C*, **78**(4) 044332.
[21] Chu, Y., Ren, Z., Dong, T., & Wang, Z. W. (2009). *Phys. Rev. C*, **79**(4) 044313.
[22] Hassan, M. A. (2010). (Doctoral dissertation, MSc. thesis, University of Baghdad, 1-80).
[23] Antonov, A. N., Nikolaev, V. A., & Petkov, I. Z. 1980 *Zeitschrift für Physik A Atoms and Nuclei*, **297**(3) 257
[24] De Vries, H., De Jager, C. W., & De Vries, C. 1987 *Data Tables*, **36**(3) 495
[25] W. Reuter, G. Fricke, K. Merle, H. Miska 1982 *Phys. Rev.* C, **26** 806
[26] Hamoudi, A. K., Flaiyh, G. N., & Mohsin, S. H. 2012 *Iraqi J. Sci.* **53**(4) 819
[27] Hamoudi, A. K., & Ojaimi, H. F. 2014 *Iraqi J. Sci.* **12**(24) 33
[28] Noori, R. I., & Ridha, A. R. 2019 *Iraqi J. Sci.* **60** (6)1286
[29] Ridha, A. R., & Abbas, Z. M. 2018 *Iraqi J. Sci.* **16**(36) 29-

[30] Ridha, A. R. (2016 *Iraqi Journal of Physics (IJP)* **14**(30) 42
[31] Ridha, A. R. (2017). *Al-Nahrain Journal of Science*, **20**(3) 83
[32] Antonov, A. N., Hodgson, P. E., & Petkov, I. Z. (2012). Springer Science & Business Media.
[33] Antonov, A. Hodgson, P. & Petkov, I. Zh. 1988. Nucleon Momentum and Density Distribution in Nuclei. Clarendon, in, Oxford.
[34] Tanihata, I., Hamagaki, H., Hashimoto, O., Nagamiya, S., Shida, Y., Yoshikawa, N., ... & Takahashi, N. (1985). *Phys. Lett. B*, **160**(6) 380
[35] Antonov, A. N., Hodgson, P. E., & Petkov, I. Z. (1993). Momentum Distributions in Nuclei. In *Nucleon Correlations in Nuclei* (pp. 111-156). Springer, Berlin, Heidelberg.